

THE FINITE ELEMENT METHOD IN ELECTROMAGNETICS

Magdalena Salazar-Palma^{*}, Luis-Emilio García-Castillo^{**}, and Tapan K. Sarkar^{***}

^{*} Dpto. Señales, Sistemas y Radiocomunicaciones, ETSI Telecomunicación
Universidad Politécnica de Madrid, Ciudad Universitaria s/n, 28040 Madrid, Spain
e-mail: m.salazar-palma@ieee.org

^{**} Dpto. Ingeniería Audiovisual y Comunicaciones, EUIT Telecomunicación
Universidad Politécnica de Madrid, Carretera de Valencia, Km. 7, 28031 Madrid, Spain
e-mail: luise@diac.upm.es

^{***} Dept. Electrical and Computer Engineering, Syracuse University
121 Link Hall, Syracuse, NY 13244-1240, USA
e-mail: tk Sarkar@mailbox.syr.edu

Key words: Complete Residual and Recovery Error Estimates, Green's Function, History of the Finite Element Method in Electromagnetics, Iterative Procedure, Nédélec's Curl-Conforming Elements, Open Problems, Self-Adaptive Mesh, Spurious Modes, Time-Domain Finite Element Method, Wavelet-Like Basis Functions.

Abstract. *This Key Note presents a summary of the development of the Finite Element Method in the field of Electromagnetic Engineering, together with a description of several contributions of the authors to the Finite Element Method and its application to the solution of electromagnetic problems. First, a self-adaptive mesh scheme is presented in the context of the quasi-static and full-wave analysis of general anisotropic multiconductor arbitrary shaped waveguiding structures. A comparison between two a posteriori error estimates is done. The first one is based on the complete residual of the differential equations defining the problem. The second one is based on a recovery or smoothing technique of the electromagnetic field. Next, an implementation of the first family of Nédélec's curl-conforming elements done by the authors is outlined. Its features are highlighted and compared with other curl-conforming elements. A presentation of an iterative procedure using a numerically exact radiation condition for the analysis of open (scattering and radiation) problems follows. Other contributions of the authors, like the use of wavelet like basis functions and an implementation of a Time Domain Finite Element Method in the context of two-dimensional scattering problems are only mentioned due to the lack of space.*

1 INTRODUCTION: DEVELOPMENT OF THE FINITE ELEMENT METHOD IN ELECTROMAGNETICS

During the 1940s and 1950s, a number of engineers in the field of structural mechanics set up the basis for the *Finite Element Method* (FEM), that was further refined during the 1960s [1, Ch. 1]. In 1965 O. C. Zienkiewicz and Y. K. Cheung used FEM to solve two-dimensional (2D) field problems derived from Poisson's equation [2]. This marked the extension of FEM to non-structural problems. A related paper for three-dimensional (3D) structures with applications to electrical problems followed [3]. The first paper to be published in a scientific journal dealing with the FEM solution of an electromagnetic wave problem (i.e., an eigenvalue problem) is due to S. Ahmed and appeared in 1968 [4]. The modes propagating along homogeneous metallic waveguides were analysed employing a scalar variational formulation in terms of the longitudinal component of either the magnetic field for transverse electric (TE) modes, or the electric field for transverse magnetic (TM) modes. First order scalar Lagrange elements were used. P. P. Silvester presented a similar study at the 1968 URSI International Symposium, but it was published in *Alta Frequenza* in 1969 [5]. Also in 1968, P. L. Arlett, A. K. Bahrani, and O. C. Zienkiewicz, published a paper applying FEM to the analysis of several homogeneous waveguides, a 3D homogeneous transducer, and a dielectric-loaded waveguide. They did not provide complete information about the formulation used for the two latter devices [6]. In 1969, higher order Lagrange elements were developed by P. P. Silvester [7], [8]. They were applied to homogeneous waveguide (eigenvalue) problems and quasi-static (deterministic) problems.

Also in 1969, S. Ahmed and P. Daly published two papers on homogeneous and inhomogeneous waveguide analysis, respectively [9], [10]. A formulation in terms of both longitudinal components was used in the latter case. Other papers using similar approaches appeared during the 1970s [11]-[14], including the analysis of anisotropic and optical waveguides [15], and lossy structures [16]. This formulation leads to the appearance of spurious modes (i.e., non-physical solutions) within the range of values of physical modes, because of the non-definite character of the operator. This fact forced the researchers to use vector formulations (i.e., in terms of vector quantities, like the electric field, the magnetic field, the transverse electric field vector, the transverse magnetic field vector, and so on), mainly, those formulations derived from the double-curl form of Maxwell's equations. As an extension of the previous FEM formulations, they were directly discretized with classical Lagrange elements by using a separate scalar approximation for each of the vector fields components (Cartesian, polar, and so on). Soon it was realised that these approaches also generated spurious modes that polluted the computed spectrum. Such modes were reported also for 3D eigenvalue problems (cavities) and 2D and 3D full-wave deterministic problems (discontinuities). Procedures were proposed to separate or distinguish them from physical solutions. Spurious modes have been a nightmare for microwave engineers and is one of the reasons for the slow development of FEM in this field. The understanding of the topic of spurious mode has been reached only recently (see the detailed account given in [1, Ch. 3 and 7] and Section 3 of this paper).

The most popular solution to the spurious modes problem is nowadays the use of vector elements, namely curl-conforming elements. During the 1970s formulations employing variables

related through constitutive laws, giving rise to mixed, dual, or hybrid FEMs were studied by a number of researcher in applied mathematics and other fields of engineering. The vector quantities involved were approximated through new vector elements (i.e., elements using vector basis functions). In 1997 P. A. Raviart and J. M. Thomas proposed 2D divergence-conforming elements [17]. In 1980 J. C. Nédélec extended them to 3D and presented also his first family of curl-conforming elements, of the type called mixed order [18]. In 1983 A. Bossavit and J. C. Verité proposed the use of Nédélec elements to solve 3D Eddy current problems [19]. In the field of microwave engineering, vector elements (however, different from Nédélec's elements) were used, for the first time, by M. Hano in 1984, who applied them to the full-wave analysis of dielectric-loaded waveguides obtaining a spurious-free mode spectrum [20]. Hano mentioned that the space spanned by the spurious modes is just the null space of the curl operator, as already noted in [21]. When Lagrange elements are used spurious modes are not correctly modelled and they appear as non-zero eigenvalue modes, while curl-conforming elements model them as numerically zero eigenvalue modes. Once the microwave community realised this fact, researchers proposed different 2D and 3D linear and higher order vector elements of both mixed and complete order type. Section 3 is devoted to this topic, and to the presentation of a practical implementation of the first family of curl-conforming Nédélec's elements done by the authors of this paper [1, Ch. 2, 3 and 7], [22]. The features and advantages of such elements as compared with other curl-conforming elements, popular among the microwave community, are presented in the context of the analysis of resonant homogeneous and inhomogeneous cavities.

The relatively reduced use of FEM for high frequency problems up to the late 1970s is due also to the difficulty on applying it to open-region problems, mainly 2D and 3D scattering and radiation problems. Due to the nature of FEM, which needs to discretize the whole domain of definition of the problem, an artificial boundary must be used to truncate the domain in order to obtain a finite number of unknowns. A boundary condition must be written over the artificial boundary that should be able to simulate the electromagnetic field behaviour on the external region; it should also produce a mesh with a low number of unknowns. In 1971 P. P. Silvester and M. S. Hsieh applied FEM to the solution of Laplace's equation over an unbounded domain using integral equations to formulate the terminating condition over the artificial boundary [22]. This approach has been termed hybrid Finite Element/Boundary Integral (FE-BI) method or simply *hybrid method*. It is one of the methods of a family that uses nonlocal boundary conditions. B. H. McDonald and A. Wexler used FE-BI to solve Helmholtz's equation over infinite domains [23]. The method provides exact radiation conditions. Thus, the artificial boundary may be close to the sources of the problem, so that a reduced number of unknowns are obtained. However, it destroys the sparse and banded nature of the FEM matrices. After those pioneering works the method has been applied to a variety of problems with different formulations and type of elements until nowadays (see an account in [1, Ch. 6]). Other nonlocal boundary conditions techniques are the hybridization of FEM with the Boundary Element Method (FEM-BEM) and the Method of Moments (FEM-MOM) [1, Ch. 6]. In 1974 M. C. Deconon employed conformal mappings to transform open quasi-static problems in closed ones [24]. Also in 1974 K. K. Mei formulated the condition over the artificial boundary using an expansion of the

equivalent sources of the problem in terms of eigenfunctions of the Helmholtz operator [25]. A drawback of these two latter methods (the conformal mapping and the *unimoment method*, respectively) is their reduced versatility, since they are advantageous mainly for problems with simple geometries. Several approaches appeared later on trying to overcome the limitations of the unimoment method (see [1, Ch. 6]).

From 1977 investigation on a different approach to solve open problems through the use of local boundary conditions was started by researchers in the field of applied mathematics [26]-[32]. These methods are also known as using *Absorbing Boundary Conditions* (ABCs). The idea underlining ABCs is to preserve the sparsity of the FEM matrices by formulating the radiation condition at the artificial boundary through differential equations. In this way the field at a given node of an element having an edge or a vertex on the artificial boundary will be related only to the field of the neighbouring nodes. However, this procedure does not provide exact radiation conditions at the near field region. Thus, the artificial boundary must be placed far away from the sources of the problem, leading to a high number of unknowns. It was not until the end of the 1980s that ABCs left the mathematical forums to start to be widely known in the engineering arena and, in particular, in computational electromagnetics. The first works in this field are due to A. F. Peterson and coworkers [33], [34]. In the latter reference a 2D scattering problem was solved employing FEM together with a Bayliss-Turkel ABC to truncate the mesh. Since then, an extensive research has been made in the development and application of both scalar and vector ABCs for the FEM solution of electromagnetic problems [1, Ch.6].

As an attempt to circumvent the problems posed by the use of ABCs, new approaches have been developed in the last few years, namely, *Numerical Absorbing Boundary Conditions* (NABCs), the *Measured Equation of Invariance* (MEI), and the *complementary operator method* [1, Ch. 6], [35]. An alternate approach, known as *Perfectly Matched Layer*, is the use of a layer of lossy material with low level of reflection to enclose the problem [1, Ch.6].

Section 4 is devoted to the description of an iterative procedure for open region problems developed by the authors [1, Ch. 6 and 7]. It combines the advantages of the nonlocal boundary procedures and the local boundary techniques, i.e., a reduced number of unknowns are obtained and the sparsity of the FEM matrices is retained. The method imposes at the artificial boundary (through a point-wise Galerkin procedure) a numerically exact radiation condition, computed through the use of the free space Green's function.

As of this date FEM has been applied to the quasi-static analysis of arbitrary-shaped inhomogeneous anisotropic multiconductor transmission lines, as well as the full-wave analysis of general waveguiding structures, including dielectric waveguides and optical fibers. Problems like discontinuities (e.g., posts, irises, junctions, bends), design of microwave devices, analysis of dielectric resonators, 2D and 3D scattering problems, antenna analysis, penetration of electromagnetic waves in biological bodies, and semiconductor devices modelling, have been successfully solved. Losses, nonlinearities, and magnetic materials have been included [36]. Nine years were required to publish the second book in FEM electromagnetics [37] after that of P. P. Silvester and R. L. Ferrari in 1983 [38]. However, since 1995 ten more books have been published

(see [1, Ch. 1] and <http://ohio.ikp.liu.se/fe/index.html>). The number of publications in scientific journals grows year by year. The leading role has been taken by the *IEEE Transactions on Magnetics*. In fact, due to its flexibility and facility in handling nonlinearities FEM became the most popular numerical tool for the low frequency, magnetics, and power engineering community after the pioneering work of [39]. Nowadays, as previously described, FEM is also well introduced in high frequency electromagnetic engineering. New types of elements and basis functions are being investigated (see, for example, [40], [41]). Cauchy's, Prony's, Padé's, matrix pencil, and similar methods are being used for efficient wideband analysis of electrically large structures. The finite element method is being applied also to time domain (FE-TDM) electromagnetic problems (see [1, Ch. 1]). The authors have also implemented a FE-TDM for the analysis of 2D scattering problems [42].

The FEM has demonstrated to be a flexible, efficient and powerful numerical tool, capable of giving highly accurate solutions if the discretization utilised (i.e., the mesh of elements in which the domain of the problem is subdivided, and the distribution of degrees of freedom over those elements) is well adapted to the solution of the problem (i.e., the electromagnetic field configuration). In fact, the FEM is generally applied in an iterative fashion. Once a computer code has been developed for the solution of a given type of problems (e.g., quasi-static or full-wave analysis of waveguiding structures, 3D resonant structures, 2D or 3D scattering or radiation devices) it is applied over an initial mesh of the structure under study. This initial discretization is devised in accordance with the researcher experience. The study of the results obtained from this first analysis allows the researcher to determine which regions of the structure should be further refined. In practice, the discretization of the domain may be the most cumbersome task of a FEM program user. Thus, automatic self-adaptive mesh techniques are highly attractive. Self-adaptive mesh procedures are based on the computation of *a posteriori* error estimates or indicators, in conjunction with adequate selective refinement strategies. The error incurred with a given mesh (in particular, an initial coarse mesh) is quantified at both the local (i.e., over each element) and the global (i.e., over the whole domain) levels. These error estimates or indicators are used to decide which regions should be enriched. The mesh is automatically refined in those areas either by subdividing each element into smaller elements (*h* refinement), increasing its order (*p* refinement), relocating the degrees of freedom (*r* refinement), or a combination of these techniques. The FEM is applied to the new mesh. The process continues until a given criterion is fulfilled. The basis of self-adaptive mesh techniques were laid by I. Babuska during the 1975 MAFELAP Conference [43]. However, in the field of electromagnetics they were not applied until mid 1980s, and they have become popular only recently. In [1, Ch. 4] the history of the development of self-adaptive mesh procedures is summarised. Section 2 of this paper is devoted to the description of a self-adaptive mesh technique implemented by the authors.

2 SELF-ADAPTIVE MESH TECHNIQUE

From 1975 a number of different *a posteriori* error estimates or indicators have been proposed [1, Ch. 4]. Among them an important group is the one formed by error estimates based on the

computation of the residue of the differential equations defining the problem, either over the domain of the element, along element boundaries, or, both in the domain and on the boundaries (complete residual). Recently, a second group of error estimates based on smoothing or recovery techniques became very popular. The error is estimated measuring the difference between the FEM solution and a more accurate solution obtained through a postprocess of the FEM solution.

The authors of this paper have implemented self-adaptive mesh algorithms based on complete residual error estimates and recovery type error estimates. Details of both procedures may be found in [1, Ch. 2] and [44], respectively. In both cases, the energy norm is used to measure the error over each element (i.e., the local error estimate or indicator). The square of the global error estimate or indicator is obtained as the sum of the square of the local ones. The global error estimate may be used to decide if a given mesh should be further refined. Then in order to decide which elements should be enriched a characteristic local error estimate is computed. Its value may be obtained as the maximum value of the local error estimates, their mean value, or their weighed value. Elements having an error estimate over a given percentage (selected by the user) of the characteristic error value are termed primary elements and would be enriched.

The refinement strategy may be to subdivide each primary element into two or more elements (h refinement), increase the order of the polynomial approximation (p refinement), relocate the nodes (r refinement), a combination of those techniques (e.g., hp refinement, hr refinement), or the generation of a new mesh [1, Ch. 4]. The procedure selected by the authors is a selective h refinement, eventually followed by a uniform p refinement.

The third important tool of a self-adaptive mesh technique is the element subdivision algorithm. In [1, Ch. 4] a number of subdivision algorithms are described. The authors have selected the method based in the bisection of the longest edge of an element [45]. In order to obtain a conforming mesh, this algorithm requires the extension of the refinement to non-primary elements contiguous to primary ones. Those elements are termed secondary elements. Figure 1 summarises this algorithm for the case of triangular meshes. ABC is a primary element, while CBD and EAC are secondary elements. The division into four elements of element ABC generates node f on the longest edge of element EAC and node g on an edge that is not the longest one of CBD. The latter element is subdivided into three elements, since its longest edge is subdivided by the line Bi and triangle BiC is subdivided by line ig. Instead EAC is divided into two elements by the line fE. This algorithm guarantees that degenerated elements will not appear. Furthermore, the transition between regions of triangles of different sizes is smooth. The refinement process does not result in an excessive number of elements.

Figure 2 (a) shows the cross section of an infinite square coaxial line. The central conductor has a potential of 1 volt with respect to the outer conductor. The energy stored by this structure may be computed analytically by means of a conformal transformation. The re-entrant corners of the inner conductor forces the electrostatic potential to behave as $r^{2/3}$ near the corners, where r stands for the distance from a corner vertex to a point close to that corner. Hence, the gradient of the potential (and, consequently, the transverse electric field) is a non-smooth vector function with a singular behaviour of type $r^{-1/3}$ near the corners.

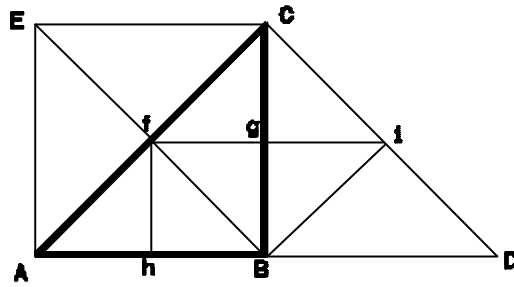


Figure 1: Illustration of the longest side bisection algorithm.

This implies that for a uniform mesh (as the initial one shown in Figure 2 (b)), the interpolation error of elements close to the corner will be much higher than the error of the other elements. Hence one would expect that a self-adaptive mesh technique should refine the region close to the corners. Figure 2 (b)-(f) shows the evolution of the mesh for the FEM quasi-static analysis of the structure, with second order Lagrange elements and the self-adaptive mesh procedure using the complete residual error estimate. A similar evolution of the mesh is obtained for the recovery error. The expected refinement at the corners is obtained.

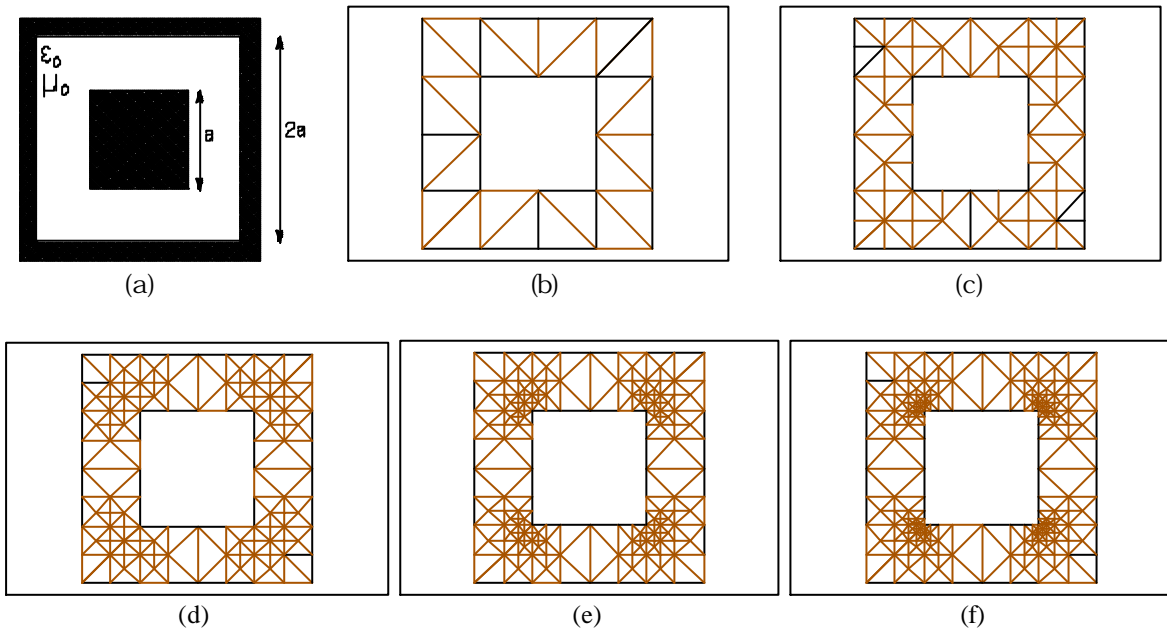


Figure 2: Square coaxial line. (a) Cross section. (b)-(f) Evolution of the mesh refinements obtained through the use of the self-adaptive mesh technique with a complete residual error estimate and second order elements.

The type of singularity of the exact solution implies also, that if uniform refinements are used, the rate of convergence will be proportional to $N_d^{-1/3}$, independently of the order of the polynomial approximation utilised. Instead, if a selective h refinement is performed so that equilibrated meshes are obtained (i.e., meshes where all local errors are of the same order of magnitude), the rate of

convergence will be proportional to $N_d^{-p/2}$, where p stands for the order of the polynomial approximation. This is the maximum rate of convergence of the FEM h version, obtained for problems with smooth exact solution using uniform refinements. Figure 3 shows results for the rate of convergence obtained for the self-adaptive mesh FEM applied to the quasi-static analysis of the square coaxial line of Figure 2. The vertical axis represents, in logarithmic scale, the energy norm of the relative error. The horizontal axis, also in logarithmic scale, represents the total number of nodes. The theoretical rates of convergence for equilibrated meshes for first and second order elements are also shown (i. e., $-1/2$ and -1 , respectively). Results for the complete residual error estimate and the recovery type error estimate are compared. It may be seen that both error estimates give the expected rate of convergence for equilibrated meshes, demonstrating the excellent performance of the self-adaptive mesh technique.

The effectivity index is defined as the ratio between the global error estimate and the energy norm of the exact error. The effectivity index of a correct self-adaptive mesh procedure should tend to unity as the number of nodes increases. Figure 4 shows the evolution of the effectivity index for the quasi-static analysis of the square coaxial line. Figure 4 refers to the case of second order elements. It may be seen how the self-adaptive procedure is correct for both error estimates in both cases.

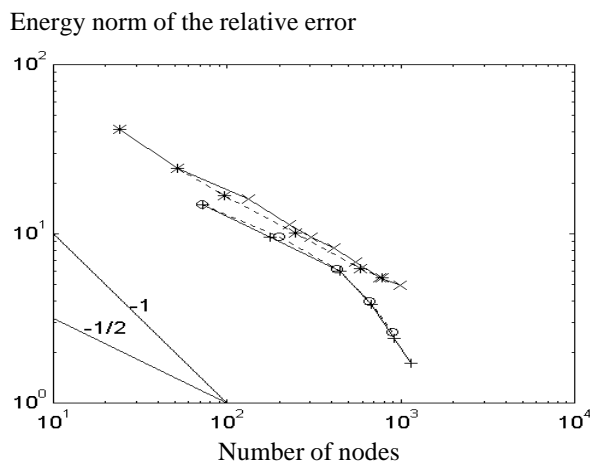


Figure 3: Rate of convergence of the self-adaptive mesh procedure applied to the quasi-static analysis of the square coaxial line. Continuous line: Recovery type error estimate. Discontinuous line: Complete residual error estimate. Marks: \times , $*$: first order elements; $+$, o : second order elements.

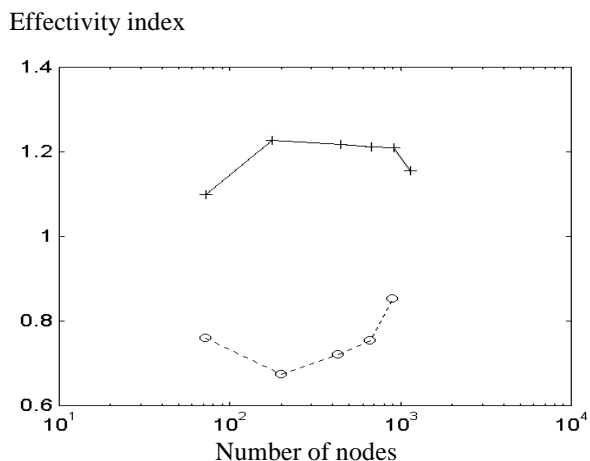


Figure 4: Evolution of the effectivity index of the self-adaptive mesh procedure applied to the quasi-static analysis of the square coaxial line. Second order elements. Continuous line: Recovery type error estimate. Discontinuous line: Complete residual error estimate.

In [1, Ch. 4 and 5] many other examples of the application of the self-adaptive mesh algorithm to the quasi-static analysis of homogeneous and inhomogeneous, isotropic and anisotropic, arbitrarily shaped multiconductor transmission line may be found. In all cases excellent results were obtained.

Figure 5 compares the fourth mesh step for the analysis of the first and second TE mode and the first TM mode of an L-shaped waveguide. A full-wave analysis together with a self-adaptive mesh technique was used. For the TE modes analysis a formulation in terms of the electric field was utilised. For the TM mode analysis a formulation in terms of the magnetic field was used. In both cases Nédélec's first family of curl-conforming vector elements were used. In Figure 5 (a) it may be seen that for the first TE mode the mesh is refined at the corner, in agreement with the singular behaviour of the electric field in the direction of the line bisecting the re-entrant corner. The second TE mode does not have a singular behaviour at the corner. Figure 5 (b) shows that the mesh does not get refined at the corner, but in the regions where the field strength is higher. The magnetic field of the first TM mode has a singular behaviour near the corner in the direction perpendicular to the bisecting line. Figure 5 (c) shows that the mesh is refined accordingly, as well as in the areas where the strength of the field is high. In [1, Ch. 4 and 5] more examples of the application of the self-adaptive mesh algorithm to the full-wave analysis of homogeneous and inhomogeneous, isotropic and anisotropic arbitrarily shaped waveguiding structures with one or more conductors may be found. In all cases excellent results were obtained with moderate CPU time.

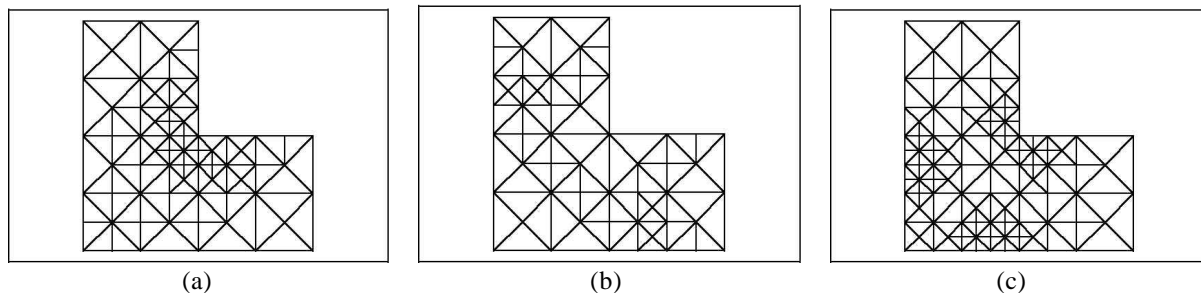


Figure 5: Fourth mesh step for the self-adaptive mesh algorithm applied to the full-wave analysis of the L shaped waveguide. (a) First TE mode. (b) Second TE mode. (c) First TM mode.

3 CURL-CONFORMING ELEMENTS AND THE SPURIOUS MODES PROBLEM

As mentioned in the introduction, the use of scalar (nodal) elements (e.g., Lagrange elements), in conjunction with double-curl formulations, produces spurious modes. In addition to the spurious modes problem, nodal elements have other drawbacks, among them an inconsistent modelling of the electric or magnetic fields at the interfaces between different materials and a complicated implementation of perfect electric or magnetic Dirichlet boundary conditions over arbitrary boundaries. These are consequences of the way in which vector quantities are discretized by means of scalar elements (i.e., each vector component is expanded in terms of scalar basis functions), in which the continuity of the vector field is imposed among elements. These problems may be always avoided but at the expense of complicating the FEM implementation.

Instead, vector elements may discretize the vector field as a whole, by means of vector basis functions. Two families of vector elements may be distinguished: elements conforming in $H(\text{curl})$ and elements conforming in $H(\text{div})$. $H(\text{curl})$ and $H(\text{div})$ are Hilbert spaces of square integrable vector functions with square integrable curl or divergence, respectively. Divergence-conforming elements provide the continuity of the vector unknown across element interfaces in the sense of the divergence

operator, i.e., normal continuity, as opposed to curl-conforming elements that provide tangential continuity, but not normal continuity. Divergence-conforming elements are suitable for the discretization of the electric and magnetic inductions, \mathbf{D} and \mathbf{B} , while curl-conforming elements are appropriate to approximate the electric and magnetic fields, \mathbf{E} and \mathbf{H} .

Different types of curl-conforming elements have appeared since Nédélec's 1980 paper [18]. It may be distinguished between mixed order elements and polynomial complete elements. Polynomial complete elements have the same order of approximation along any direction. An example is the Nédélec second family in 3D proposed in 1986 [46], based on the work of F. Brezzi et al [47]. Mixed order elements (e.g., those of Nédélec's first family) provide a constrained representation of the vector field leading to a different order of polynomial approximation along one direction than along the others.

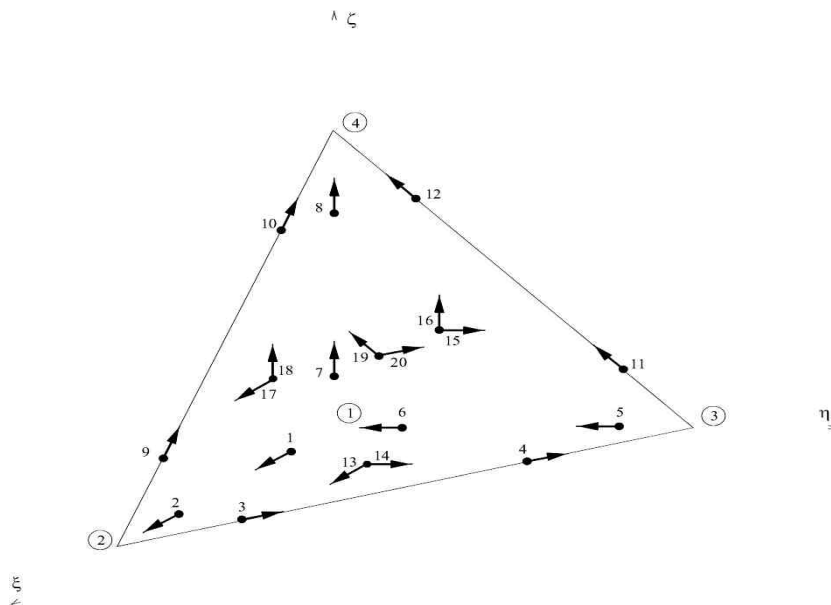
The reasons for using a constrained approximation of the field are the following. Spurious modes correspond to numerical approximations of non-physical solutions of the FEM differential formulation of the problem. Non-physical solutions are allowed to exist because of the lack of enforcement of some of the Maxwell's equations. In particular, the divergence-free condition and its associated boundary conditions are not, either explicitly or implicitly, present in double-curl formulations for $\omega=0$. Therefore, non-physical solutions may exist corresponding to $\omega=0$, i.e., to static solutions, when double-curl formulations are employed. In other words, the non-physical modes belong to the null space of the curl operator and hence they can be derived as the gradient of a scalar function, i.e. of a potential. When these static solutions are not properly modelled, as it happens to be with nodal elements, they appear as non-zero eigenvalue spurious modes in the discretized problem. Hence, they pollute the spectrum. However, when curl-conforming elements are employed, non-physical solutions are properly modelled and they appear as numerically zero eigenvalue modes. Thus, the spurious modes may be easily distinguished from the physical solutions. In fact spurious modes do not pollute the spectrum. The number of spurious modes, i.e., the number of zero eigenvalues in the discretized problem depends on the order and types of polynomial functions involved in the discretization. In particular, mixed order elements of order $k+1$ (i.e., with rate of convergence of order $k+1$) yield the same number of spurious modes that a complete order element of order k (i.e., with rate of convergence of order k). Hence, for a given order, mixed order elements are more efficient in terms of the number of degrees of freedom actually used in the approximation of non-zero curl vector fields, i.e., of physical solutions.

The constrained representation of the field was proposed by Nédélec for his first family of curl-conforming elements [18] and hence, these constraints are referred to as Nédélec's constraints. The first order Nédélec element has been widely utilised by the electromagnetic FEM community. It is known as edge element because, in this case, only degrees of freedom related to the edges of the element are defined. Namely, the degrees of freedom are proportional to the tangential component of the field at the edges. Unlike for the first order case, the degrees of freedom of higher order elements are not only associated with the edges of the mesh, but also with the faces and the volume of the element. The mathematics behind the higher order elements are considerable more complex than for the first order case. In addition, Nédélec's paper [18] does not explicitly show the basis functions, but just the mathematical definition of the finite element (the space of basis functions and the general

definition of the degrees of freedom as linear operators). Therefore, the practical FEM implementation of the higher order Nédélec elements has led to different elements.

In this context, several higher order curl-conforming elements have appeared claiming to follow Nédélec's pioneering work and hence, yielding to mixed order elements. However, although some of those elements show a constrained representation of the field as proposed by Nédélec, they are not rigorously Nédélec elements because they do not follow the definition of the basis functions or/and the degrees of freedom given by Nédélec. The higher order triangular and tetrahedral element implementations proposed by the authors follow rigorously Nédélec's element definition. Details may be found in [1, Ch.2, 3, and 7], [22] and will not be repeated here. In summary there are two types of degrees of freedom: either related to the boundary of the element or to the inner domain of the element. The former ones are basically defined in terms of momenta of the tangential component of the vector unknown over the element boundary. The latter are defined in terms of momenta of the vector unknown over the area (2D case) or volume (3D case) of the element. As a consequence of those definitions the vector basis functions are all of the same order k , i.e., the order of the element. This is not the case for other mixed order curl-conforming elements appeared in the literature (e.g., [48], [49]). Those elements span the same space of vector functions. However, the definition of the degrees of freedom that they use leads to a set of basis functions where only few of them are of order k , while the other are of order $k-1$. This fact is reflected by the condition number of the FEM matrices, which is worse than in the case of the elements implemented by the authors.

As an example of the performance of the implementation of Nédélec's mixed order curl-conforming elements done by the authors, several results obtained with the second order tetrahedron (Figure 6) are shown. It has been employed, in conjunction with a double-curl vector formulation, to find the resonance modes of inhomogeneous and arbitrarily shaped 3D cavities. The formulation may



be written in terms of the electric field or the magnetic field. Figure 6: Second order curl-conforming tetrahedral element: 20 degrees of freedom: 2 per edge, 2 per facet.

First, results of an empty rectangular cavity of dimensions $1 \times 0.5 \times 0.75$ are presented. It is chosen because of the availability of analytic solutions. The convergence study has been made for the first mode, TE_{z101} , using a uniform refinement of the mesh. The rate of convergence of the second order element is compared with the rate of convergence achieved with the first order element (i.e., the edge element). In particular, meshes with discretizations of $1 \times 1 \times 1$, $2 \times 1 \times 2$, $4 \times 2 \times 4$, $8 \times 4 \times 8$, cubes per coordinate axis (x, y, z , respectively) are employed for the first order case. The tetrahedrons are obtained by subdividing each cube into six tetrahedrons. In the case of the second order element, the discretization employed is of $2 \times 1 \times 2$, $4 \times 2 \times 4$, $8 \times 4 \times 8$ cubes. Figure 7 (a) compares the rate of convergence for the eigenvalue (k_o^2 , where k_o stands for the vacuum wave number) obtained with first and second order tetrahedral elements with the theoretical one ($-2/3$ and $-4/3$, respectively). A good agreement is observed.

A rectangular cavity of dimensions $1 \times 0.1 \times 1$ with a dielectric (of relative permittivity $\epsilon_r=2$) in the upper half part has been chosen as an example of an inhomogeneous structure. A convergence study has been made for the first mode, which has zero amplitude variation along y direction. Uniformly refined meshes of $2 \times 1 \times 2$, $4 \times 2 \times 4$ and $8 \times 4 \times 8$ cubes per coordinate axis are employed for the first order case, while meshes with $2 \times 1 \times 2$, $4 \times 2 \times 4$, $6 \times 3 \times 6$ and $8 \times 4 \times 8$ cubes are used for the second order case. An adapted mesh refinement has been also used with first order elements. Namely, meshes of $2 \times 1 \times 2$, $4 \times 1 \times 4$, $6 \times 1 \times 6$, $8 \times 1 \times 8$ and $10 \times 1 \times 10$ cubes have been utilised. It is worth noting that with the adapted refinement all meshes have just one cube in the y direction, due to the null variation of the first mode along it. Figure 7 (b) shows the comparison between the rate of convergence of the eigenvalue obtained with the second order and the first order Nédélec tetrahedrons. A good agreement between the obtained rates of convergence and the theoretical ones is observed. Also, it is interesting to check the superconvergence behaviour corresponding to the first order elements using adapted meshes, which equals the rate of convergence obtained with the second order elements and uniform mesh refinement.

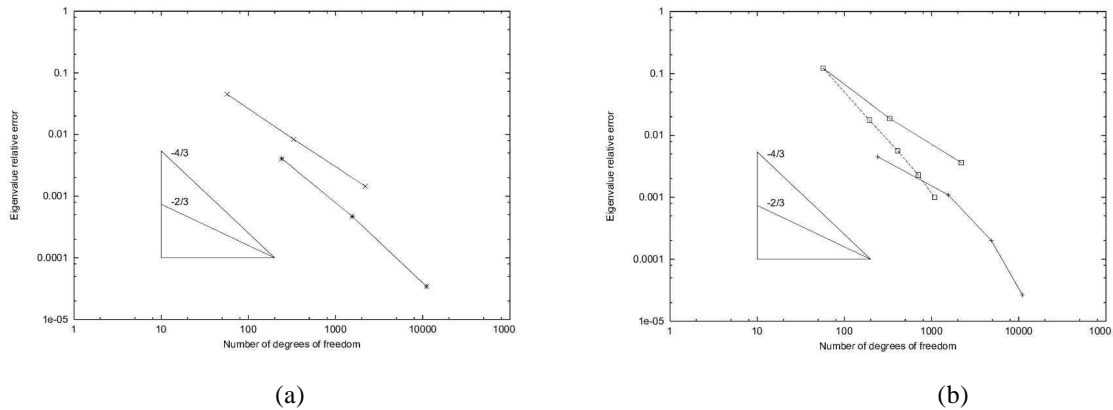


Figure 7: Rate of convergence of k_o^2 for: (a) Empty cavity. \times : First order elements. $*$: Second order elements. (b) Half-filled cavity. Squares: First order element. Continuous line: uniform refinements. Discontinuous line: adapted mesh. $+$: Second order elements.

A comparison of the condition number of the mass matrix of the tetrahedral second order curl-conforming element developed by the authors and other second order elements appeared in the literature [48], [49], is presented in Table 1. The condition number has been computed as the ratio of the maximum and minimum eigenvalues. The mass matrix (i.e., the matrix whose coefficients are the inner product between the FEM basis functions) has been computed over the parent element. It may be observed how the condition number in the case of the element developed by the authors is one order of magnitude lower than those of [48] and [49].

	$\lambda_{\max}/\lambda_{\min}$
Second order Nédélec element implemented by the authors	137
[48]	1337
[49]	1907

Table 1: Condition number for the mass matrix of the parent element.

Other examples of the application of Nédélec's curl-conforming elements may be found in [1, Ch. 3, 4, 5 and 7]. Triangular elements have been used for the full-wave analysis of arbitrarily shaped, multiconductor, anisotropic, inhomogeneous waveguiding structures. Tetrahedral elements were used for the analysis of discontinuities and other 3D problems.

4 ITERATIVE PROCEDURE FOR THE SOLUTION OF OPEN PROBLEMS

As mentioned in the introduction, the authors have developed an iterative method that combines the advantages of the FE-BI methods with the ABCs [1, Ch. 6 and 7]. The method makes use of the boundary integral representation of the exterior field to truncate the mesh but at the same time it does retain the banded and sparse structure of the FEM matrices. This is achieved at the expense of performing a number of iterations. At each iteration, the boundary condition at the artificial boundary is imposed as a point-wise Dirichlet condition for the FEM formulation. The Dirichlet boundary condition is computed using the Green's function and the Equivalence Principle over the FEM solution of the previous iteration. In addition, its implementation is very simple. The analysis of open region problems may be easily incorporated in existing FEM computer codes for non-open region problems.

The basis of the method is described in the following. Consider an open region problem, e.g., a scattering or a radiation problem. It may include different anisotropic materials, conducting objects, and symmetry walls. An artificial boundary S is used to close the problem (see Figure 8). The closed domain, bounded by the surface S , is referred to as Ω . This is the domain used in the FEM analysis. Therefore, the domain Ω is meshed and FEM equations are written inside it. This method has been applied to 2D electrostatic problems, 2D scattering problems (namely, to the TM or TE scattering from perfectly conducting cylinders, using a scalar formulation in terms of the longitudinal electric or magnetic field, respectively) and to 3D full-wave scattering and radiation (antenna) problems. The description of the method given here, is focused on the last application: full-wave analysis of 3D scattering and radiation problems. In this case, a full-wave double-curl formulation in terms of the

electric (or the magnetic) field has been used, in conjunction with tetrahedral curl-conforming elements. However, the philosophy of the method is independent of the formulation and the type of elements used. The only requirement is that the FEM equations in the near field region (i.e., in the region enclosed by S) should be written accordingly to the formulation of the problem considered.

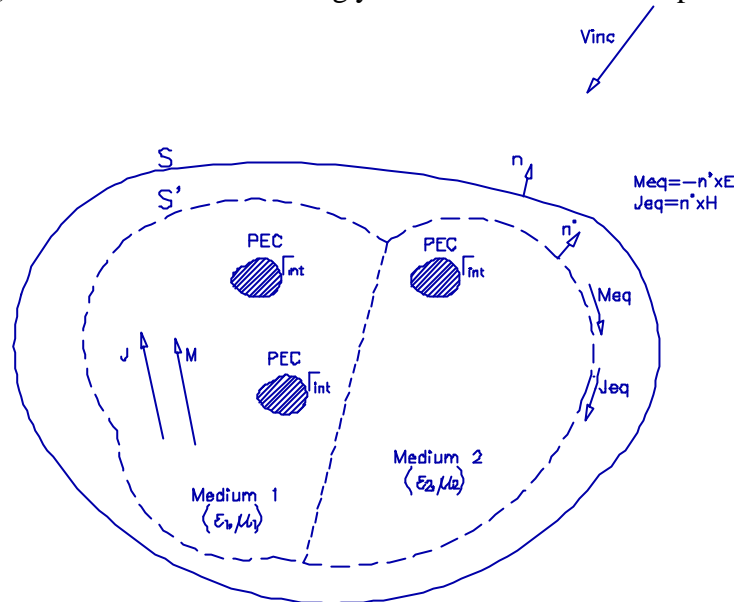


Figure 8: Illustration of an open-region problem. Scattering and radiation.

The next step is the solution of the FEM system of equations. First, it is necessary to provide a boundary condition on S in order to define uniquely the problem. Here is the key of the method. The values of the degrees of freedom on S are supposed to be known, i.e., when solving the FEM system of equations the boundary condition on S must be imposed as a Dirichlet boundary condition (in a point-wise fashion). For the first iteration, the degrees of freedom on S are fixed to some initial values. For curl-conforming elements, the degrees of freedom on S are related to the tangential components of the field. Thus, they are made equal to zero for a radiation problem (or a formulation in terms of the scattered field, in the case of a scattering problem), or, they are given a value proportional to the tangential component of the incident field, in the case of the total field formulation of a scattering problem.

After imposing in the FEM system the values of the degrees of freedom on S , the FEM system is solved. This may be done through the use of any direct or iterative (e.g., conjugate gradient) solver. Making use of the Equivalence Principle, equivalent sources (electric and magnetic currents in the case that is been considered) are computed over an auxiliary surface S' (see Figure 8), as a postprocess of the FEM solution. Outside S' these equivalent sources provide the same field as that of the original sources (within S'). Inside S' the total field of the equivalent problem is zero. The auxiliary surface S' is placed in such a way that it encloses all non-homogeneities and conducting objects, and possible internal sources (e.g., as in the case of a radiation problem). Thus, the value of the field outside S' could be computed from the free-space Green's function. In particular, the free-space Green's function is utilised to obtain updated values of the degrees of freedom on the external

boundary S , i.e., the values of the tangential field at the nodes placed on S .

These updated values of the degrees of freedom on S will be, in general, different from those values used previously to terminate the FEM mesh. In that case, a new iteration will take place. The updated values of the degrees of freedom on S are used as new point-wise Dirichlet boundary conditions on S . The FEM system with these new values for the boundary condition is solved again and new equivalent sources will be computed. Note that the new iteration starts in step vi of Table 2, i.e., it is not necessary to fill the FEM matrix again. The solution of the FEM system in step vii can be done efficiently either with a direct or an iterative solver. Observe that the matrix $[K'']$ may be the same for all iterations. Only $\{F''\}$ needs to be updated. Thus, if a direct solver is utilised the factorization of $[K'']$ (which is the most computation intensive process) can be performed only once at the first iteration. The system is solved at subsequent iterations by simple back-substitution. For the iterative method the solution of the previous iteration may be used as an initial guess for the next iteration. The process continues until an error criterion is satisfied (e.g., the difference between the values of the degrees of freedom on S between two consecutive iterations).

Step	Operation
i)	Mesh the domain Ω enclosed by S
ii)	Obtain the FEM discrete integral forms in each element
iii)	Assemble the element discrete forms \Rightarrow Global FEM discrete form $\{W\} = [K]\{D\} - \{F\}$
iv)	Enforce the boundary conditions not related to $S \Rightarrow \{W\} = [K']\{D\} - \{F'\}$
v)	Choose the initial values for the degrees of freedom on S
vi)	Enforce the values of the degrees of freedom on $S \Rightarrow \{W''\} = [K'']\{D\} - \{F''\}$
vii)	Solve the FEM system $[K'']\{D\} = \{F''\}$
viii)	Compute the equivalent sources on surface S' from the FEM field solution
ix)	Compute the new values of the degrees of freedom on S from the equivalent sources and the Green's function
x)	Check the error criteria between two consecutive sets of values of the degrees of freedom on S
xi)	If error criteria is satisfied, then stop. If not, continue from step vi) with the last set of values of degrees of freedom on S computed in ix)

Table 2: Summary of the iterative method for the analysis of open-region problems

Thus, the method leads to sparse matrices and, at the same time, provides an accurate radiation boundary condition when the artificial surface S is placed close to the original sources of the problem. Indeed, the radiation boundary condition is satisfied exactly, in a numerical sense, through the use of the Green's function. It is worth noting that the problem with an open region has been reduced to perform a set of solutions of Maxwell's equations in a closed domain Ω subject to Dirichlet and Neumann boundary conditions. Thus, the structure of the FEM system corresponding to the open-region problem (at each iteration cycle) is identical to that of a closed-region problem. This has some important advantages. First of all, it allows the use of sparse solvers for the solution of FEM systems, with the corresponding saving in storage and CPU resources. On the other hand, as mentioned before, the analysis of open-region problems may be incorporated very easily in existing FEM computer codes for non open-region problems. In fact, only two subroutines should be added. The first one is the computation of the equivalent sources, from the FEM solution. The second one is the computation of the degrees of freedom on S , from the computed equivalent currents and the free-

space Green's function.

To illustrate the performance of the method two simple examples have been chosen. First, a dipole antenna is analysed. Figure 9 shows the schematic of the configuration of the meshes used for its analysis. The rectangular artificial boundary S encloses the dipole. The auxiliary surface S' where the equivalent currents are calculated, is chosen to be rectangular. The distance $S-S'$ is $0.1\lambda_0$ (where λ_0 is the free-space wavelength) and the distance between the dipole and S' varies between $0.05\lambda_0$ and $0.1\lambda_0$. The excitation of the problem is a unit amplitude z -directed volumetric (square cross sectional cylinder) electric current \mathbf{J} located at the dipole. Three different lengths of the dipole are considered: $0.1\lambda_0$, $0.5\lambda_0$, and $1\lambda_0$. The meshes used for the analysis lead to 1854, 2592, and 6144 nodes, respectively. Figure 10 shows the latter one. Both formulations, in terms of the electric or the magnetic field, have been used. A comparison of the far-field solution corresponding to the preceding three cases is shown in Figure 11 for the case of the \mathbf{H} formulation. A good agreement with the analytic solutions is observed. The evolution of the error for the $0.1\lambda_0$ dipole is shown in Figure 12. The convergence is achieved in four and five iterations for the magnetic and electric field formulations, respectively.

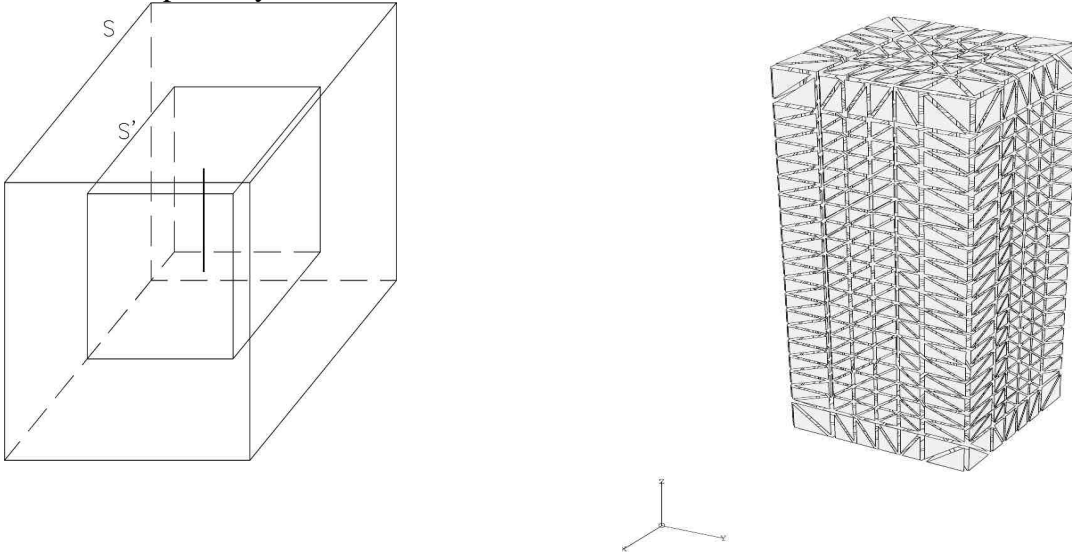


Figure 9: Configuration of the dipole problem. Figure 10. Mesh for the case of dipole length λ_0 .

As an example of a scattering problem, consider the scattering from an anisotropic dielectric cube. The anisotropic material is characterized by a symmetric relative permittivity tensor ($\epsilon_{rxx}=4.0$, $\epsilon_{ryy}=3.5$, $\epsilon_{rzz}=4.5$, $\epsilon_{rxy}=0.5$, $\epsilon_{ryz}=0.5$, $\epsilon_{rxz}=0.5$). Figure 13 shows the configuration of the problem. A unit amplitude plane wave coming from ($\theta_i=90^\circ$, $\phi_i=0^\circ$) is assumed. Two different polarizations are considered in the y - and z -directions. The normalized scattered field obtained

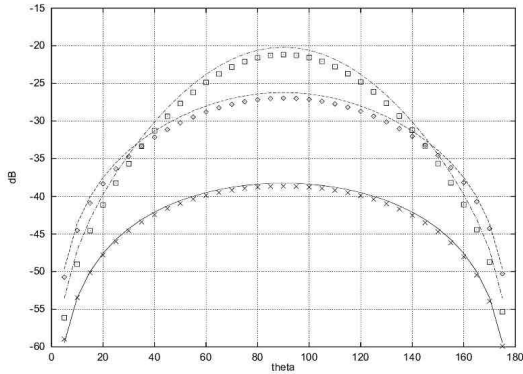
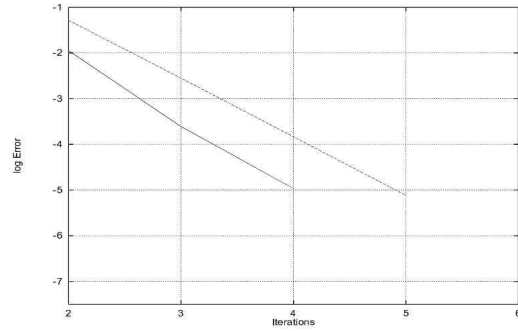


Figure 11: Far field (dB), **H** formulation ($\phi = 0^\circ$).
Lines: analytic results (—: $0.1\lambda_0$, - - : $0.5\lambda_0$, - . - : λ_0).



Marks: this method.
Figure 12: Relative error on S.
—: **H** formulation. - - : **E** formulation.

with the **H** formulation is shown in Figure 14. The anisotropic case is compared with the isotropic case ($\epsilon_r = 4$). Again, the convergence is achieved in few iterations. The smooth curve corresponds to the case of the polarization in the z -direction, while the curve with the dip is obtained with the y -polarized wave. As expected, the behaviour of the scatterer is slightly different depending on the polarization. In Figure 14 it may be observed that the curve with the dip (y -polarization) shifts downward when the anisotropic case is considered. The opposite happens with the smooth curve (z -polarization), which is shifted upward. This is due to the smaller value of $\epsilon_{r_{yy}}$ and the larger value of $\epsilon_{r_{zz}}$, respectively, compared with the isotropic case ($\epsilon_r = 4$). Also, a shift in the location of the dip is observed.

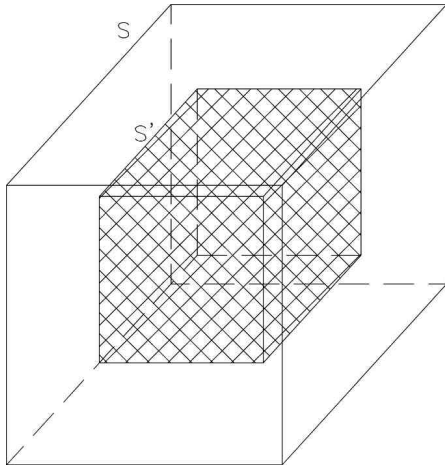


Figure 13: Configuration of the dielectric cube problem.

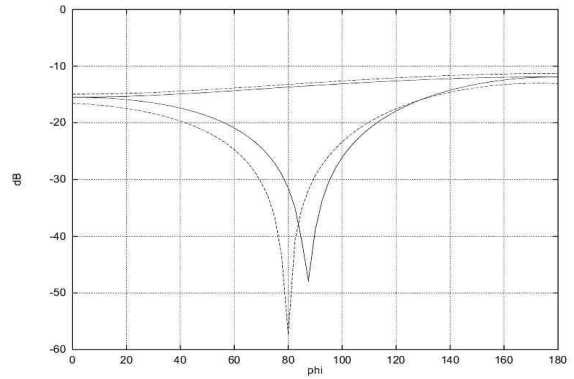


Figure 14: Scattered field (dB) ($\theta=90^\circ$).
—: isotropic. - - : anisotropic.

In [1, Ch. 6 and 7] other 2D and 3D open-region problems are considered. In all cases excellent results are obtained.

4 CONCLUSIONS

This Key Note Paper has presented a summary of the development of FEM in the field of high frequency electromagnetics, with special emphasis in the spurious mode problem and open-region problem analysis. The Finite Element Method is nowadays well introduced in the field of microwaves and millimeter wave and is recognised as a powerful and flexible numerical tool that can provide accurate solutions for many electromagnetic problems with moderate computational time. A number of contributions of the authors have been highlighted. Among them, a self-adaptive mesh procedure, the implementation of higher order curl-conforming elements of Nédélec's first family, and an iterative procedure for the solution of open-region problems. All three techniques have demonstrated excellent performances. Other important contributions of the authors are the use of wavelet-like basis functions, in order to obtain a high percentage of diagonalization of the FEM matrices, and a Finite Element Time Domain Method for scattering problems.

ACKNOWLEDGEMENTS

This work has been partially financed by the Comisión Interministerial de Ciencia y Tecnología (Spain), projects TIC-96-0724-C06 and TIC-99-1172-C02-01.

REFERENCES

- [1] M. Salazar-Palma, T. K. Sarkar, L.-E. García-Castillo, T. Roy, A. Djordjevic, *Iterative and Self-Adaptive Finite-Elements in Electromagnetic Modeling*, Ed. Artech House, Inc., Norwood, MA, USA, 1998.
- [2] O. C. Zienkiewicz, Y. K. Cheung, "Finite Elements in the Solution of Field Problems", *The Engineer*, 1965, vol. 200, pp. 507-510.
- [3] O. C. Zienkiewicz, P. L. Arlett, A. K. Bahrani, "Solution of Three Dimensional Field Problems by the Finite Element Method", *The Engineer*, 1967, vol. 224, pp. 547-550.
- [4] S. Ahmed, "Finite Element Method for Waveguide Problems", *Electronics Letters*, 1968, vol. 4, pp. 381-389.
- [5] P. P. Silvester, "Finite Element Solution of Homogeneous Waveguide Problems", *Alta Frequenza*, 1969, vol. 38, pp. 313-317.
- [6] P. L. Arlett, A. K. Bahrani, O. C. Zienkiewicz, "Application of Finite Elements to the Solution of Helmholtz Equation", *Proc. IEE*, 1968, vol. 115, pp. 1762-1766.
- [7] P. P. Silvester, "A General High-Order Finite Element Waveguide Analysis Program", *IEEE Trans. Microwave Theory Tech.*, 1969, vol. MTT-17, pp. 204-209.
- [8] P. P. Silvester, "High-Order Polynomial Triangular Finite Elements for Potential Problems", *Int. J. Eng. Science*, 1969, vol. 7, pp. 849-861.
- [9] S. Ahmed, P. Daly, "Waveguide Solutions by Finite Element Method," *Radio Electron Eng.*, 1969, vol. 38, pp. 217-223.
- [10] S. Ahmed, P. Daly, "Finite-Element Methods for Inhomogeneous Waveguides," *Proc. IEE*, 1969, vol. 116, pp. 1661-1664.
- [11] Z. J. Csendes, P. P. Silvester, "Numerical Solution of Dielectric Loaded Waveguides: I — Finite Element Analysis," *IEEE Trans. Microwave Theory Tech.*, 1970, vol. MTT-18, pp. 1124-1131.
- [12] Z. J. Csendes, P. P. Silvester, "Numerical Solution of Dielectric Loaded Waveguides: II — Modal

- Approximation Technique," *IEEE Trans. Microwave Theory Tech.*, 1971, vol. MTT-19, pp. 504–509.
- [13] Z. J. Csendes, P. P. Silvester, "Dielectric Loaded Waveguide Analysis Program," *IEEE Trans. Microwave Theory Tech.*, 1971, vol. MTT-19, p. 789.
- [14] P. Daly, "Hybrid-Mode Analysis of Microstrip by Finite-Element Methods," *IEEE Trans. Microwave Theory Tech.*, 1971, vol. MTT-19, pp. 19–25.
- [15] P. Vandenbulcke, P. E. Lagasse, "Eigenmode Analysis of Anisotropic Optical Fibers or Integrated Optical Waveguides," *Electronics Letters*, 1976, vol. 12, pp. 120–122.
- [16] A. D. McAulay, "Variational Finite-Element Solution for Dissipative Waveguides and Transportation Application," *IEEE Trans. Microwave Theory Tech.*, 1977, vol. MTT-25, pp. 382–392.
- [17] P. A. Raviart, J. M. Thomas, "A Mixed Finite Element Method for 2nd Order Elliptic Problems," in *Mathematical Aspects of the Finite Element Method*, Eds. I. Galligani, and E. Mayera, Lect. Notes on Mathematics, 1977, vol. 606, Springer-Verlag, New York, pp. 293–315.
- [18] J. C. Nédélec, "Mixed Finite Elements in R^3 ," *Numer. Math.*, 1980, vol. 35, pp. 315–341.
- [19] A. Bossavit, J. C. Verité, "A Mixed FEM-BIEM Method to Solve 3-D Eddy Current Problems," *IEEE Trans. Magnetics*, 1982, vol. 18, pp. 431–435.
- [20] M. Hano, "Finite-Element Analysis of Dielectric-Loaded Formulation in Terms of the Magnetic Field Vector for Dielectric Waveguides," *IEEE Trans. Microwave Theory Tech.*, 1984, vol. MTT-32, pp. 1275–1279.
- [21] M. Hara, T. Wada, T. Fukasawa, F. Kikuchi, "A Three-Dimensional Analysis of RF Electromagnetic Fields by the Finite Element Method," *IEEE Trans. Magnetics*, 1983, vol. MAG-19, pp. 2417–2420.
- [22] L. E. García-Castillo, M. Salazar-Palma, "Second-Order Nédélec Tetrahedral Element for Computational Electromagnetics," *International Journal of Numerical Modelling: Electronic Networks, Devices and Fields*, 2000, vol. 13, pp. 261–287.
- [22] P. P. Silvester, M. S. Hsieh, "Finite-Element Solution of 2-Dimensional Exterior-Field Problems," *IEE Proc.*, 1971, vol. 118, pt. H, pp. 1743–1747.
- [23] B. H. McDonald, A. Wexler, "Finite-Element Solution of Unbounded Field Problems," *IEEE Trans. Microwave Theory Tech.*, 1972, vol. MTT-20, pp. 841–847.
- [24] M. C. Decreton, "Analysis of Open Structures by Finite-Element Resolution of Equivalent Closed-Boundary Problem," *Electronics Letters*, 1974, vol. 10, pp. 43–44.
- [25] K. K. Mei, "Unimoment Method of Solving Antenna and Scattering Problems," *IEEE Trans. Antennas Propag.*, 1974, vol. AP-22, pp. 760–766.
- [26] B. Engquist, B. A. Majda, "Absorbing Boundary Conditions for the Numerical Simulation of Waves," *Math. Comp.*, 1977, vol. 31, pp. 629–651.
- [27] A. Bayliss, E. Turkel, "Radiation Boundary Conditions for Wave-Like Equations," *Comm. Pure Appl. Math.*, 1980, vol. 33, pp. 107–125.
- [28] G. Mur, "Absorbing Boundary Conditions for the Finite-Difference Approximation of the Time-Domain Electromagnetic-Field Equations," *IEEE Trans. Electromagnetic Compat.*, 1981, vol. EC-23, pp. 377–382.
- [29] A. Bayliss, M. Gunzburger, E. Turkel (1982), "Boundary Conditions for the Numerical Solution of Elliptic Equations in Exterior Regions," *J. Appl. Math.*, 1982, vol. 42, pp. 430–451.
- [30] A. Bayliss, C. I. Goldstein, E. Turkel, "On Accuracy Conditions for the Numerical Computation of Waves," *J. Comp. Physics*, 1985, vol. 59, pp. 396–404.
- [31] L. N. Trefethen, L. Haalpern, "Well-Posedness of One-Way Wave Equations and Absorbing Boundary Conditions," 1986, vol. 47, pp. 421–453.
- [32] J. G. Blaschak, G. A. Kriegsmann, "A Comparative Study of Absorbing Boundary Conditions," *J. Comp. Physics*, 1988, vol. 77, pp. 109–139.
- [33] A. F. Peterson, "Absorbing Boundary Conditions for the Vector Wave Equation," *Microwave Optical Tech. Letters*, 1988, vol. 1, pp. 62–64.
- [34] A. F. Peterson, S. P. Castillo, "A Frequency-Domain Differential Equation Formulation for Electromagnetic Scattering from Inhomogeneous Cylinders," *IEEE Trans. Antennas Propag.*, 1989, vol.

- AP-37, pp. 601–607.
- [35] G. K. Gothard, S. M. Rao, T. Roy, T. K. Sarkar, M. Salazar-Palma, "Finite Element Solution of Open Region Problems Incorporating the Measured Equation of Invariance," *Microwave and Guided Wave Letters*, 1995, vol. 5, pp. 252–254.
- [36] R. Coccioli, T. Itoh, G. Pelosi, P. P. Silvester, "Finite Element Methods in Microwaves: A Selected Bibliography," *IEEE Antennas Propag. Magazine*, 1996, vol. 36, pp. 34–48.
- [37] M. Koshiba, *Optical Waveguide Theory by the Finite Element Method*, K. T. K. Scientific Publishers, Tokyo, 1992.
- [38] P. P. Silvester, R. L. Ferrari, *Finite Elements for Electrical Engineers*, Cambridge University Press, Cambridge, 1983.
- [39] P. P. Silvester, M. V. K. Chari, "Finite Element Solution of Saturable Magnetic Field Problem," *IEEE Trans. Power Appl. Syst.*, 1970, vol. PAS-89, pp. 1642–1651.
- [40] T. K. Sarkar, R. S. Adve, L. E. García-Castillo, M. Salazar-Palma, "Utilization of Wavelet Concepts in Finite Elements for an Efficient Solution of Maxwell's Equations," *Radio Science*, 1994, vol. 29, pp. 965–977.
- [41] T. K. Sarkar, C. Su, R. Adve, M. Salazar-Palma, L. E. García-Castillo, R. Rodríguez-Boix, "A Tutorial on Wavelets from an Electrical Engineering Perspective, Part 1: Discrete Wavelet Techniques", *IEEE Antennas and Propagation Magazine*, vol. 40, no. 5, Oct. 1998, pp. 49- 70.
- [42] T. K. Sarkar, T. Roy, M. Salazar-Palma, A. R. Djordjevic, "Finite-Element Time Domain Method", Ch. 8 in *Time Domain Electromagnetics*, Ed. S. M. Rao, Academic Press, San Diego, CA, USA, 1999, pp. 279–305.
- [43] I. Babuska, "The Selfadaptive Approach in the Finite Element Method", in *The Mathematics of Finite Elements and Applications II, MAFELAP 1975*, Ed. J.R. Whiteman , Academic Press, New York, 1976, pp. 125-142.
- [44] M. Salazar-Palma, L.-E. García-Castillo, A. Bocigas-Palma, T. K. Sarkar, "A Comparison between Different Self-Adaptive Schemes in the Application of the Finite Element Method to Electromagnetic Problems", *XXVIth General Asseembly of the International Union of Radio Science*, Toronto, Canada, Aug. 13-21, 1999.
- [45] M. C. Rivara, P. Inostroza, "Using Longest-Side Bisection Techniques for the Automatic Refinement of Delaunay Triangulation", *Int. J. Numer. Meth. Eng.*, 1997, vol. 40, pp. 581-598.
- [46] J. C. Nédélec, "A New Family of Mixed Finite Elements in \mathfrak{R}^3 ", *Numer. Math.*, 1986, vol. 50, pp. 57-81.
- [47] F. Brezzi, J. Douglas, Jr., L. D. Marini, "Two Families of Mixed Finite Elements for Second Order Elliptic Problems," *Numer. Math.*, 1985, vol. 47, pp. 217–235.
- [48] J. F. Lee, D. K. Sun, Z. J. Csendes, "Tangential Vector Finite Elements for Electromagnetic Field Computation", *IEEE Trans. Magnetics*, 1991, vol. MAG-27, no. 5, pp.4032-4035.
- [49] J. S. Savage, A. F. Peterson, "Higher-Order Vector Finite Elements for Tetrahedral Cells", *IEEE Trans. Microwave Theory Tech.*, 1996, vol. MTT-44, no.6, pp. 874-879.